

Journal of Computations & Modelling, vol.8, no.3, 2018, 1-16
ISSN: 1792-7625 (print), 1792-8850 (online)
Scienpress Ltd, 2018

Estimation of a coefficient of the Hamilton-Jacobi equation by using adjoint methods

Abani Maidaoua Ali¹, Bisso Saley² and Benjamin Mampassi³

Abstract

We are interested to the coefficient of the non-linear convection term estimation of the Hamilton-Jacobi equation, in two-dimensional, with the Cauchy-Dirichlet conditions. We validate numerically some properties of the KPZ equation with the same conditions mention above while making a correlation with the surface-growth phenomenon.

Mathematics Subject Classification: 35F21; 34K29; 65N35; 49J20; 35K55

Keywords: Hamilton Jacobi equation; Inverse problem; Pseudo-spectral method; Optimal control; KPZ-equation

¹ Dpartement de Mathmatiques et Informatiques, Universit Dan Dicko Dankoulodo de Maradi (Niger). E-mail: indice002@yahoo.fr

² Dpartement de Mathmatiques et Informatiques, Universit Abdou Moumouni (Niger). E-mail: bsaley@yahoo.fr

³ Dpartement de Mathmatiques et Informatiques, Universit Cheikh Anta Diop de Dakar (Sinigal). E-mail: mampassi@yahoo.fr

1 Introduction

We use the compact adjoint technique to estimate the parameter "a" , which is the coefficient of the convection term of the Hamilton-Jacobi problem defined by:

$$\begin{cases} \frac{\partial u}{\partial t} - \Delta u = a |\nabla u|^p & \text{in } \Omega \times]0, +\infty[\\ u = 0 & \text{on } \partial\Omega \times]0, +\infty[\\ u(\cdot, 0) = u_0 & \text{in } \bar{\Omega} \end{cases} \quad (1)$$

where $a \in \mathbb{R}$, $a \neq 0$ and Ω is a bounded open subset of \mathbb{R}^2 .

The technique we used belong to the family of the variational methods based on the optimal control theory [2],[3],[10],[11],[16],[18], [20],[22], [27]. We manually generate the compact adjoint codes by using the spectral method based on the Chebyshev points [24], [26]. Such an approach is proved to be very efficient in the inverse problems resolution, governed by partial differential equations (PDE) [12]. We carried out the various simulations in MatLab. There are automatic differentiation packages that generate the associated codes. However, those developed in MatLab require refinement [23], [25].

Several works have been done in the setting of the existence and uniqueness of solution of the Hamilton-Jacobi problem [4],[5],[8],[9],[13],[19],[21].

We also conduct the numerical study of the problem (1) when $a = 1$ and $p = 2$, corresponding to the KPZ problem which translate the surface-growth phenomenon [8],[9],[14],[15],[28].

This work is organized as follows: In the first section we present the inverse problem formulation that permits to estimate the parameter "a" of (1). In the second section, we conduct the numerical scheme validation and verify numerically some theoretical results as the solution extinction, in finite time, of the Cauchy-Dirichlet problem of the KPZ equation. In the last section, we present numerical simulations of the parameter estimation.

2 Inverse problem formulation

Let's consider the functional

$$J_\lambda(a) = \frac{1}{2} \int_0^T \|\Lambda.S(a;t) - U^{obs}\|_{\mathcal{O}}^2 dt + \frac{\lambda}{2} \|a - a^b\|^2. \quad (2)$$

where \mathcal{O} is the observation space, Λ is the observation operator, U^{obs} is the observation, and a^b is the first guess.

The problem is to minimize the functional (2) under constraint (1). We use the variational data assimilation techniques based on the compact adjoint method [1].

By using a partial discretization in space, the problem (1) drives us to an ordinary differential equation of the shape

$$\begin{cases} \frac{dU}{dt} = F(U, a), & t \in]0, T[\\ U(0) = u \end{cases} \quad (3)$$

where $U(t)$ is the state belonging to the Hilbert space $\mathcal{H} \equiv \mathbb{R}^N$.

We get the complete numerical scheme by using the explicit Euler method:

$$\begin{cases} U_{k+1} = U_k + \Delta t F(U_k, a), & k = 0 : M - 1 \\ U_0 = u \end{cases} \quad (4)$$

where U_k is the approximation vector of $U(t)$, solution of the problem (3), in \mathbb{R}^N at the time $t_k = k\Delta t$. Let's denote by \mathcal{P} the admissible space of the estimate parameter and $a \in \mathcal{P}$. Let's make the following hypothesis:

Hypothesis 2.1. *Given $a \in \mathcal{P}$ and $T > 0$, we assume that there exists a unique function $U \in \mathcal{H}$, solution of the problem (3), which depends continuously on the parameter "a". Otherwise, the application*

$$\begin{aligned} S : \mathcal{P} &\longrightarrow \mathcal{H} \\ a &\longmapsto S(a) = U(a; t) \end{aligned}$$

is continuous for all $t \in [0, T]$.

Hypothesis 2.2. *We assume that the application S is Frchet differentiable for all $t \in [0, T]$. In particular, for all $\delta a \in \mathcal{P}$ and for all $t \in [0, T]$:*

$$U(a + \delta a; t) = U(a; t) + D_U(a; t) \cdot \delta a + o(\|\delta a\|_{\mathcal{P}})$$

where $D_U(a; t)$ is the derivative of the state $U(t)$ at the point a .

For the purposes of numerical processing it should be assumed that \mathcal{O} is a finite dimensional vector space or a subset of a finite dimensional vector space. Under the hypothesis 2.1, the solution of the Cauchy problem (3)

$$U(a; t) = S(a)$$

leads us to

$$U_k = S_k(a) \quad (5)$$

solution of the discrete system (4), where (S_k) is a sequence of operators which for the parameter a associates the discrete solution at the instant t_k with

$$S_0(a) = \underline{u}. \quad (6)$$

3 Numerical schemes validation

In this section, we conduct an analysis of the stability of our numerical schemes. This analysis is useful in particular for a variational assimilation problem which we will expose further in this work. We also perform numerical simulations of the KPZ problem which translate the water surface-growth phenomenon, as well as some related theoretical results.

3.1 Numerical scheme of the direct problem

To validate the numerical scheme of the problem (1), we use a "synthetic" exact solution. This aspect imposes us a source function $f(x, y, t)$. Therefore, we consider the problem

$$\begin{cases} \frac{\partial u}{\partial t} - \Delta u = a |\nabla u|^p + f(x, y, t) & \text{in } \Omega \times]0, +\infty[\\ u = 0 & \text{on } \partial\Omega \times]0, +\infty[\\ u(., 0) = u_0 & \text{in } \overline{\Omega} \end{cases} \quad (7)$$

We choose $p = 2$, $a = -1$ and $\overline{\Omega} = [-1, 1] \times [-1, 1]$.

f is defined by:

$$f(x, y, t) = \pi (\sin(\pi x) \sin(\pi y) - \cos^2(\pi x) \sin^2(\pi y) - \sin^2(\pi x) \cos^2(\pi y)) \exp(-\pi^2 t).$$

Thus, the problem (7) admits

$$u(x, y, t) = \frac{1}{\pi} \sin(\pi x) \sin(\pi y) \exp(-\pi^2 t) \quad (8)$$

as analytic solution, where the initial condition is

$$u_0(x, y) = \frac{1}{\pi} \sin(\pi x) \sin(\pi y).$$

For the discretization, we used, for the variable space (x, y) , the Chebyshev spectral method and the explicit Euler method in time. Then (7) implies

$$\begin{cases} S_{k+1}(a) = S_k(a) + \Delta t(D_{xx} + D_{yy})S_k(a) \\ \quad + a\Delta t \text{diag}(D_x S_k(a))D_x S_k(a) \\ \quad + a\Delta t \text{diag}(D_y S_k(a))D_y S_k(a) + \underline{f}, \quad k = 0, \dots, M-1 \\ S_0(a) = \underline{u}. \end{cases} \quad (9)$$

Before conducting the data assimilation, we first analyse and validate the numerical schemes stability. To analyze the numerical stability of the scheme (9), we perform numerical simulations of the exact solution (8) and the approximate solution from (9). The results of these simulations are presented in Figure 1 and the estimation of error in the table 1.

The different simulations (Figure 1) show that the numerical scheme (9)

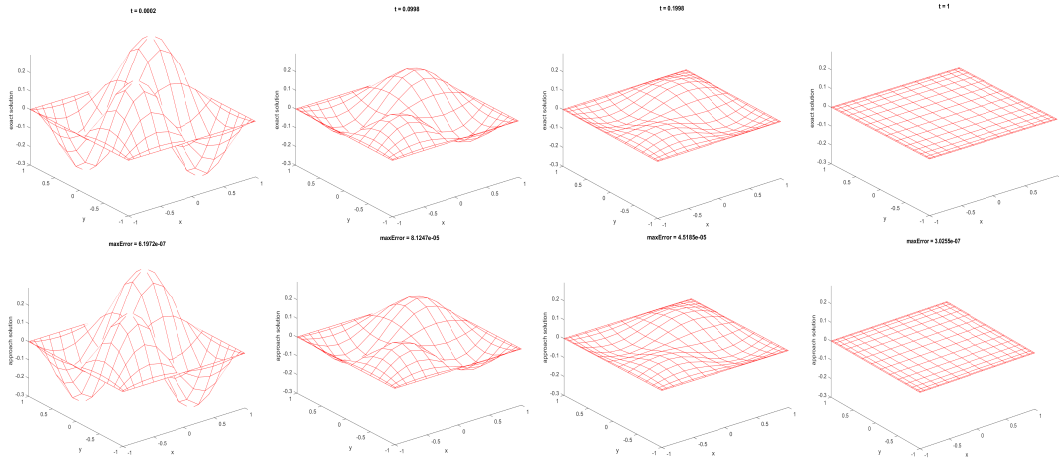


Figure 1: *Evolution of the exact solution (first line) and the approximate solution (second line).*

gives a good approximation of the exact solution (8), the error between the two solutions converges toward 0 with an optimal order in L^∞ . In fact, in general, the maximum error (infinite norm) according to the different simulations is of the order 10^{-7} (table 1). We can draw the following conclusions:

Table 1: *Estimation of error between exact and approximate solutions.*

iteration	1	3000	4000	4500	5000
Error L_∞	6.1972e-07	2.3161e-06	8.2056e-07	4.9795e-07	3.0255e-07

1. The choice of the pseudo-spectral discretization scheme allowed us to directly establish a numerical scheme of the problem (7) in matrix form. This method makes it possible to reduce the use of the loop "for" in our algorithm. Thus, we gain in computing time and storage.
2. The explicit Euler scheme with time, with a judicious choice of discretization steps $\Delta t = 0,0002$, guarantees a numerical stability of the scheme (9).

3.2 Application to the KPZ equation

Assuming $a = 1$ and $p = 2$, the problem (1) corresponds to

$$\begin{cases} \frac{\partial u}{\partial t} - \Delta u = |\nabla u|^2 & \text{in } \Omega \times]0, +\infty[\\ u = 0 & \text{on } \partial\Omega \times]0, +\infty[\\ u(., 0) = u_0 & \text{in } \bar{\Omega} \end{cases} \quad (10)$$

known as the Cauchy-Dirichlet problem of the KPZ equation. In practice, the problem (10) can reflect the phenomenon of the surface growth (shallow water for example). $u(x, y, t)$ represents the surface height's, at time t and at the point $(x, y) \in \Omega \subset \mathbb{R}^2$.

We numerically validate the extinction of the solution in finite time whatever the initial condition randomly chosen. This translates, in practice, whatever the disturbance carried out at the level of the water surface, at the initial time t_0 , the surface stabilizes horizontally at the absence of a permanent source of disturbance.

Consider a unit cubic vase filled with water at a height h_0 which representing the observation origin of the surface u in $\bar{\Omega} = [-1, 1]^2$. At rest, this surface u is in the horizontal plane passing through the origin $h_0 = 0$. By making the following assumptions:

1. the water quantity is invariant;
2. the non-existence of a permanent source of disturbance of this water;
3. the initial condition u_0 of the problem (10) represents the water surface behavior following a sudden disturbance at the initial time t_0 .

Then this surface $u(x, y, t)$ is between the two horizontal planes passing through the global extrema of u_0 . It covers its state $u = 0$ in finite time. We find explicitly (Figure 2) this phenomenon through different simulations of the numerical scheme of the problem (10).

This gives the mathematical result as follows. Assuming $a = 1$ and $p = 2$ for all initial condition u_0 , the problem (10) admits a unique classical solution $u \in C^{2,1}(\Omega \times (0, T))$ ([5],[19]) satisfying

$$\min_{\Omega} u_0 \leq u(x, y, t) \leq \max_{\Omega} u_0, \quad (x, y, t) \in [-1, 1]^2 \times [0, \infty[.$$

It's possible to prove that this solution converges towards a stable state, the null function. In the practical case, relating to the water surface growth, this stable state is reached and we have $u \equiv 0$ in $[-1, 1]^2 \times [0, \infty[$ in the absence of a permanent perturbation source. $u \equiv 0$ represents the water surface state at rest.

Remark 3.1. *Even if the boundary conditions are not Dirichlet type, the behavior of the solution remains valid [7].* ■

We give an extinction property in finite time of the solution of the problem (10).

Theorem 3.2. *Assume that $a = -1$, $p = 2$ and the initial condition u_0 depend on a bounded Random measure in $\bar{\Omega} = [-1, 1]^2$. Denoting by u the corresponding classical solution of (10),*

- 1.

$$\min_{\Omega} u_0 \leq u(x, y, t) \leq \max_{\Omega} u_0, \quad (x, y, t) \in \bar{\Omega} \times [0, \infty[.$$

2. there exists $T^* > 0$ such that

$$u(x, y, t) = 0 \text{ for each } (x, y, t) \in \Omega \times (T^*, +\infty). \quad (11)$$

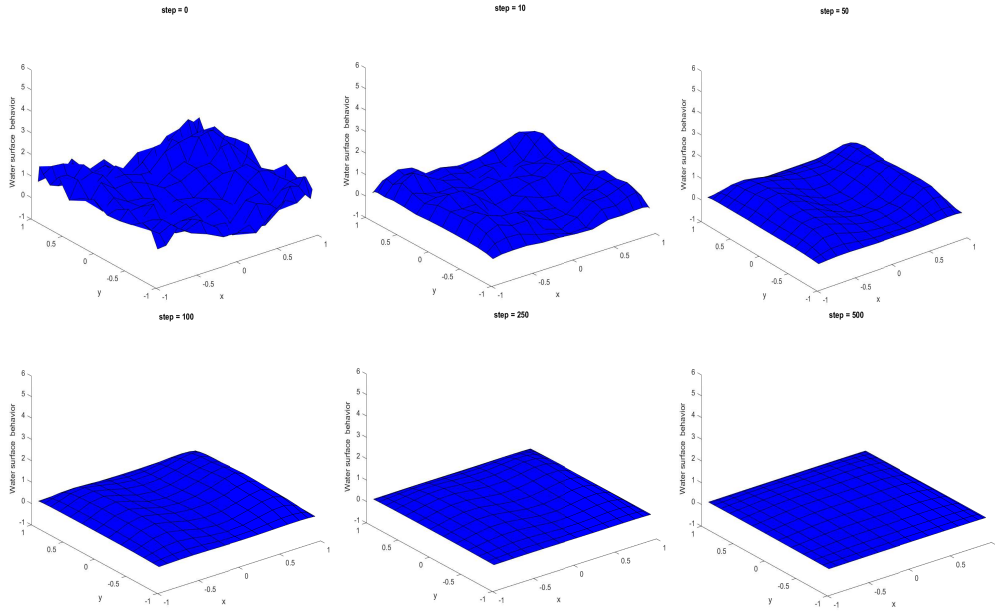


Figure 2: *Behavior of the water surface after a sudden disturbance at the initial time.*

For proof, it suffices to realize, in practice, whatever the initial condition u_0 , at a certain time t^* , $u(x, y, t^*)$ belongs to $C_0(\overline{\Omega})$. Thus, one can have a frame of the solution.

When $p = 2$, global solutions converge to zero in $L^\infty(\Omega)$ as time goes to infinity and this property remains true for all global solutions which are bounded in $C^1(\overline{\Omega})$ when $p \in (1, 2]$.

For more detail, we can refer to [5], [6], [7],[8],[17]. ■

After this result, we proceed to present the numerical scheme of the inverse problem.

3.3 Numerical scheme of the inverse problem

We have developed a compact adjoint technique for the numerical resolution of inverse problems in [1]. such an approach is proved to be very efficient in the approximation of solution of inverse problems governed by the partial differential equations (PDE), especially for the schemes which combine the pseudo-spectral methods and the compact approach of adjoint codes determination .

The discrete analog of the functional (2) can be written as follows:

$$J(a) = \frac{1}{2} \Delta t \sum_{k=0}^{M-1} \left\| \Lambda_N \cdot S_{k+1}(a) - U_{k+1}^{obs} \right\|^2 + \frac{\lambda}{2} \left\| a - a^b \right\|^2 \quad (12)$$

where Λ_N is the discrete observation operator, a^b is a background estimate of parameter a , U_k^{obs} is the observation vector at the time t_k of the state variable U . Let \tilde{a} denote a perturbation on a , then the calculation of the directional derivatives at (4) gives us the discrete tangent linear model

$$\begin{cases} \hat{U}_{k+1} &= \hat{U}_k + \Delta t \hat{F}_U \cdot \hat{U}_k + \Delta t \hat{F}_a \cdot \tilde{a}, \quad k = 0 : M - 1 \\ \hat{U}_0 &= 0 \end{cases} \quad (13)$$

where $\hat{F}_U = \frac{\partial F}{\partial U}(U_k)$ and $\hat{F}_a = \frac{\partial F}{\partial a}(U_k)$, the directional derivative of the cost function J can be expressed as follows:

$$\hat{J}(a) \cdot \tilde{a} = \Delta t \sum_{k=0}^{M-1} \langle \Lambda_N^T \cdot (\Lambda_N \cdot S_{k+1}(a) - U_{k+1}^{obs}), \hat{U}_{k+1} \rangle + \lambda \langle a - a^b, \tilde{a} \rangle. \quad (14)$$

We can determine the gradient of the functional if we succeed to express the linearity of $\hat{J}(a) \cdot \tilde{a}$. To achieve this, we calculate a scalar product of each member of (13) by q_k (adjoint state) and we make the summation of the terms. Which gives us:

$$\sum_{k=0}^{M-1} \langle \hat{U}_{k+1}, q_k \rangle = \sum_{k=0}^{M-1} \langle \hat{U}_k, q_k \rangle + \Delta t \sum_{k=0}^{M-1} \langle \hat{F}_U \cdot \hat{U}_k, q_k \rangle + \Delta t \sum_{k=0}^{M-1} \langle \hat{F}_a \cdot \tilde{a}, q_k \rangle$$

which is written again after reduction

$$\sum_{k=0}^{M-1} \langle \hat{U}_{k+1}, q_k - q_{k+1} - \Delta t \hat{F}_U^* \cdot q_{k+1} \rangle = -\langle \hat{U}_M, q_M \rangle - \langle \hat{U}_M, \hat{F}_U^* \cdot q_M \rangle + \Delta t \sum_{k=0}^{M-1} \langle \tilde{a}, \hat{F}_a^* \cdot q_k \rangle. \quad (15)$$

If one defines the adjoint q_k of \hat{U}_k as solution of the following system

$$\begin{cases} \frac{q_k - q_{k+1}}{\Delta t} - \hat{F}_U^* \cdot q_{k+1} &= \Lambda_N^T \cdot (\Lambda_N \cdot S_{k+1}(a) - U_{k+1}^{obs}), \quad k = 0 : M - 1 \\ q_M &= 0, \end{cases} \quad (16)$$

then equation (15) becomes

$$\sum_{k=0}^{M-1} \langle \hat{U}_{k+1}, \Lambda_N^T \cdot (\Lambda_N \cdot S_{k+1}(a) - U_{k+1}^{obs}) \rangle = \Delta t \sum_{k=0}^{M-1} \langle \hat{F}_a^* \cdot q_k, \tilde{a} \rangle \quad (17)$$

and the directional derivative of the cost function can be written:

$$\begin{aligned}\widehat{J}(a).\tilde{a} &= \langle \nabla_a J, \tilde{a} \rangle \\ &= \lambda \langle a - a^b, \tilde{a} \rangle + \Delta t \sum_{k=0}^{M-1} \langle \widehat{F}_a^* . q_k, \tilde{a} \rangle\end{aligned}\quad (18)$$

We deduce the gradient:

$$\nabla_a J = \lambda(a - a^b) + \Delta t \sum_{k=0}^{M-1} \widehat{F}_a^* . q_k \quad (19)$$

Remark 3.3. *The discrete scheme chosen in this part is the explicit Euler method. Another choice (implicit Euler, leap-frog, ...) would have resulted in a solution expressed differently. ■*

In this approach, to determine the gradient of the functional with respect to the control variable, it is sufficient to solve the direct model (4), then solve the adjoint model (16) and finally apply the formula (19) to have the gradient. This procedure is performed by solving the following optimality system:

$$\left\{ \begin{array}{lcl} U_0 & = & \underline{u} \\ U_{k+1} & = & U_k + \Delta t F(U_k, a) \\ \frac{q_k - q_{k+1}}{\Delta t} - \widehat{F}_U^* . q_{k+1} & = & \Lambda_N^T . (\Lambda_N . S_{k+1}(a) - U_{k+1}^{obs}) \\ q_M & = & 0 \\ \nabla_a J & = & \lambda(a - a^b) + \Delta t \sum_{k=0}^{M-1} \widehat{F}_a^* . q_k \end{array} \right. \quad (20)$$

Remark 3.4. *It is possible to transform a sub-constrained optimization problem into an unrestrained optimization problem that can be solved with relatively conventional and high-performance algorithms (such as the descent algorithm). The method consists of adding the state equation as a constraint of the cost function to be minimized. The function J and its augmented Lagrangian will have the same extrema. We can show that we achieve the same result by using the Lagrangian. ■*

3.4 Gradient test

In the optimization mechanism, it is necessary to correctly evaluate the gradient of the cost function with respect to the control variable in order to

obtain the correct descent direction. The accuracy of the gradient calculation acts on the speed of the minimization convergence and the exact value of the optimal control parameter. For this, we check the accuracy of the calculation of the gradient obtained before starting the optimization step.

The first order of the Taylor's expansion allows, in an efficient way, to validate experimentally the accuracy of the gradient. In fact, for a perturbation $v \in \mathbb{R}^N$ in the direction \tilde{w} , chosen so that $\|\tilde{w}\| = 1$, the Taylor development at the point w is given by:

$$J(w + v) = J(w) + \langle \nabla J(w), v \rangle + o(\|v\|). \quad (21)$$

Therefore, if for any direction $\tilde{w} \in \mathbb{R}^N$, we have

$$\lim_{\xi \rightarrow 0} \rho(\xi) = \lim_{\xi \rightarrow 0} \frac{J(w + \xi \tilde{w}) - J(w)}{\xi \langle \nabla J(w), \tilde{w} \rangle} = 1, \quad (22)$$

the gradient test is checked, linearization of the direct code is correct.

The gradient test algorithm: Let us note by **D** the direct code and **AD** the adjoint code. Let U be an input vector of **D** and $V = \mathbf{D}(U)$ an output vector. Let M be an integer.

Validation can be achieved through the following algorithm:

1. execute the direct code $V_0 = \mathbf{D}(U)$;
2. calculate $J_0 = J(V_0)$;
3. calculate the cost function gradient ∇J_0 by executing **AD**;
4. for $i=1:M$
 - $\xi = 2^{-i}$;
 - calculate $V_\xi = \mathbf{D}(U + \xi \delta v)$ by executing the direct code;
 - calculate $J_\xi = J(V_\xi)$;
 - evaluate the quantity

$$\rho(\xi) = \frac{J_\xi - J_0}{\xi \langle \nabla J_0, \delta v \rangle}. \quad (23)$$

The gradient test is satisfied in the direction δv if $\rho(\xi)$ converge towards 1 when i becomes large. In practice, after increasing convergence towards 1, there is a perturbation around 1. One of the results of this test is presented in Table 2. When ξ varies from 2^{-2} to 2^{-40} , the function $\rho(\xi)$ tends to 1.

Table 2: *Gradient test with $\xi \rightarrow 0$.*

ξ	$\rho(\xi)$	ξ	$\rho(\xi)$	ξ	$\rho(\xi)$
2^{-2}	0.373700210353322	2^{-15}	1.001014920052647	2^{-28}	1.001087251476291
2^{-3}	0.697737981268313	2^{-16}	1.001050737137807	2^{-29}	1.001087219853407
2^{-4}	0.851921740138193	2^{-17}	1.001068645442983	2^{-30}	1.001088389900115
2^{-5}	0.927122123615446	2^{-18}	1.001077599115940	2^{-31}	1.001087915556855
2^{-6}	0.964257670860460	2^{-19}	1.001082077938499	2^{-32}	1.001083235370023
2^{-7}	0.982710300924212	2^{-20}	1.001084316230316	2^{-33}	1.001100817693525
2^{-8}	0.991907956573396	2^{-21}	1.001085430936977	2^{-34}	1.001070712707960
2^{-9}	0.996499635322196	2^{-22}	1.001085991872587	2^{-35}	1.001115743694772
2^{-10}	0.998793689397904	2^{-23}	1.001086286484221	2^{-36}	1.000918416898628
2^{-11}	0.999940270354718	2^{-24}	1.001086409022897	2^{-37}	1.000894130523718
2^{-12}	1.000513449343803	2^{-25}	1.001086485609569	2^{-38}	1.000979132835903
2^{-13}	1.000800010971361	2^{-26}	1.001086518220668	2^{-39}	1.000938655544386
2^{-14}	1.000943284765760	2^{-27}	1.001086508338517	2^{-40}	1.000728173628499

Table 2 guarantees a convergence of the quotient (23) to the real number 1. After the gradient test, we proceed to the estimation process of the coefficient a by using the descent optimization algorithm.

4 Parameter estimation

The stop criterion considered in our optimization algorithm is based on an increase of the gradient norm. We consider the first guess value $a^b = -1,01$ and the reference value $a_{ref} = -1$. We generated the observations U_k^{obs} , following the twin experiments method, using a_{ref} and disturbing the condition U_0 .

The principle is to find an excellent estimate of the parameter a whose ideal would be a_{ref} .

Starting from the initialization value

1. $a_0 = -1.5$ we find an estimate $a = -1.000069027494187$ after 131 iterations;
2. $a_0 = -0.7$ we find an estimate $a = -0.995544157558389$ after 119 iterations.

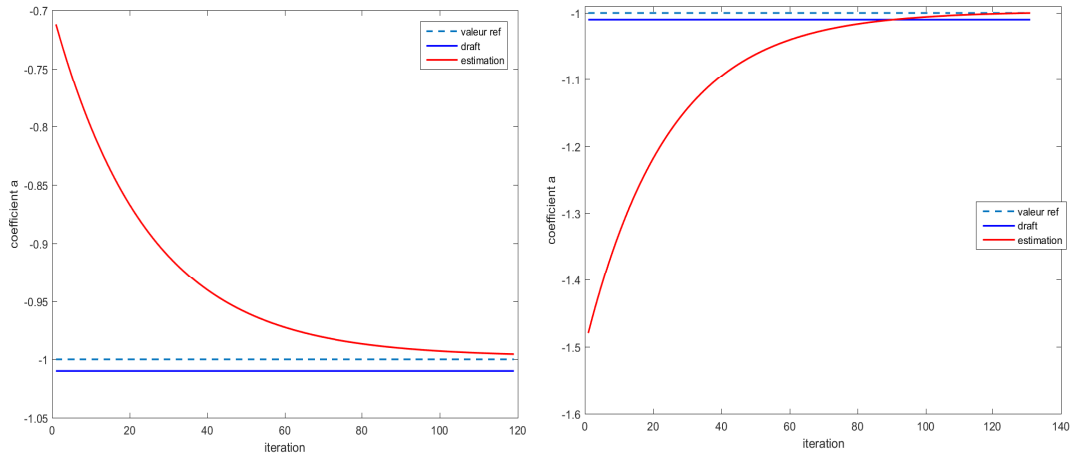


Figure 3: *Convergence of the coefficient a towards -1 .*

The figures (Figure 3), according to the iterations, show that the curve of the parameter a is asymptotic to the horizontal line passing through -1 , independently of the initialization value a_0 position. By making a comparison of the absolute errors between the reference value a_{ref} and the estimate of a , and between the first guess a^b and the estimate of a . We get the results in table 3.

Table 3: *Errors comparison.*

Initialization value: a_0	Estimate: a	$r_1 = a_{ref} - a $	$r_2 = a^b - a $
-1,5	-1,0001	0,0001	0,0099
-0,7	-0,9955	0,0045	0,0145

This table shows that a converges towards the reference value a_{ref} but not towards the first guess a^b .

References

- [1] Abani M. A.;Mampassi B.; Bisso S.; Ntaganda J. M., *Solving some non linear PDEs inverse problems variational data assimilation*, Int. J. Differ. Equ. Appl. 13,No.3,93-107 (2014).
- [2] Alexander A. S. and Peter N. V., *Numerical Methods for Solving Inverse Problems of Mathematical Physics*, Walter de Gruyter, Berlin (2007).
- [3] Andreas K., *An Introduction to the Mathematical Theory of Inverse Problems*, Springer, (2011).
- [4] Barles G. and Da Lio F., *On the generalized Dirichlet problem for viscous Hamilton-Jacobi equations*, J. Math. Pures Appli. 83(1), 53-75, (2004).
- [5] Benachour S. and Dabuleanu S.,*The mixed Cauchy-Dirichlet problem for a viscous Hamilton-Jacobi equation*, Adv. Differential Equations, 8:1409-1452, (2003).
- [6] Benachour S. and Dabuleanu S. and Laurent Ph.,*Decay estimates for a viscous Hamilton-Jacobi equation with homogeneous Dirichlet boundary conditions*, Asymptot. Anal. 51(3-4), (2007) 209-229.
- [7] Benachour S., Philippe L. and Didier S., *Extinction and decay estimates for a viscous Hamilton-Jacobi equation in \mathbb{R}^N* , AMS,Vol. 130, No 4, pp 1103-1111, (2001).
- [8] Brian H. G., *The Cauchy problem for $u_t = \Delta u + |\nabla u|^q$, large time behaviour*, J. Math. Pures. Appl. 84 (2005) 753-785.
- [9] Brian H. G. Mohammed G. Robert K., *The Cauchy problem for $u_t = \Delta u + |\nabla u|^q$* , J. Math. Appl. 284 (2003) 733-755.
- [10] Dariusz U., *Optimal Measurement Methods for Distributed Parameter System Identification*, CRC PRESS, (2005).
- [11] Donald E. Krirk, *Optimal Control Theory: An Introduction*, Mineola, N.Y. 11501, (2004).
- [12] Evans L. C., *Partial Differentiel Equations*, AMS , 1997 (T).

- [13] Jos M. A., Anibal R-B, Philippe S., *Boundedness of Global Solutions for Nonlinear Parabolic Equations Involving Gradient Blow-up Phenomena*, Ann. scuola Norm. Sup. Pisa Cl. Sci. (5) Vol.III (2004),pp. 1-15.
- [14] Kardar M., Parisi G., Zhang Y. C., *Dynamic scaling of growing interfaces*, Phys. Rev. Lett. 56(1986) 889-892.
- [15] Krug J. and Spohn H., *Universality classes for deterministic surface growth*, Phys. Rev. A. (3) 38 (1988) 4571-4283.
- [16] Lions J. L., *Optimal Control Of Systems Governed by Partial Differential Equations*, Springer-Verlag Berlin Heidelberg New York, (1971).
- [17] Michael G. C. and al., *User's guide to viscosity solutions of second order partial differential equations*, Bull. Amer. Math. Soc. (N.S.), 27(1): 1-67, (1992).
- [18] Mu M. and Jiafeng W., *A Method for Adjoint Variational Data Assimilation with Physical On Off Processes*, American Meteorological Society, volume 60 (2003) 2010-2018.
- [19] Philippe L., *Convergence to steady states for one-dimensional viscous Hamilton-Jacobi Equation with Dirichlet Boundary conditions*, pacific journal of mathematics, vol 230, No 2,(2007).
- [20] Pierre Ngnepieba et al., *Identification de paramtres: une application l'equation de Richards*, Projet idopt, lmc-imag (UJF), Volume 1-2002. arima, p. 127-157.
- [21] Quittner P. and Souplet Ph., *Superlinear parabolic problems. Blow-up, global existence and steady states*, Birkhuser Verlag, Basel, (2007).
- [22] Seon K. Park. Liang Xu, *Data Assimilation for Atmospheric, Oceanic and Hydrologic Applications*, Springer (2009).
- [23] Sylvie T., Fouad B. and Charles S., *YAO: Un logiciel pour les modes numeriques et l'assimilation de donnees*, Unit Mixte de Recherche 7159 cnrs/ird/ Universit Pierre et Marie Curie (2006)

- [24] Teng-Yao K., Hsin-Chu C. and Tzyy-Leng H., *A fast poisson solver by Chebyshev pseudospectral method using reflexive decomposition*, Taiwanese Journal of Mathematics, Vol. 17, No. 4, pp. 1167, (2013).
- [25] Thomas F. Coleman and Arun Verma, *ADMAT: An Automatic Differentiation Toolbox for MATLAB*, Siam (2000).
- [26] Trefethen Lloyd N., *Spectral Methods in Matlab*, Computer Science Department, Cornell University, Ithaca NY 14850 (1998).
- [27] Victor Isakov, *Inverse Problems for Partial Differential Equations*, Springer (2006).
- [28] Zhenli X., Houde H. and Xiaonan W., *Numerical Method for Deterministic Kardar-Parisi-Zhang Equation in Unbounded Domains*, Commun. Comput. Phys., Vol. 1, No. 3, pp. 479-493 (2006)